Simulation of Electron Scattering using Monte Carlo Methods

Thomas Graul

under the direction of
Dr. Timothy Gay
University of Nebraska-Lincoln
Department of Physics and Astronomy

August 22, 2016

1 Introduction

Although inefficient and computationally intensive, Monte Carlo simulations allow the modeling of varied physical phenomena with an accuracy dependent on the number of random events sampled. In our case, as in many, algorithms built from known probability distributions are an alternative to the approximation of solutions to differential equations that often lack explicit, analytically derived solutions. In particular with these methods, we are interested in modeling the propagation of electrons through a chamber of Nitrogen molecules and Rubidium atoms in order to optimize the transmittance of electrons with identical spin polarization. Figure 4 depicts one such electron propagation path.

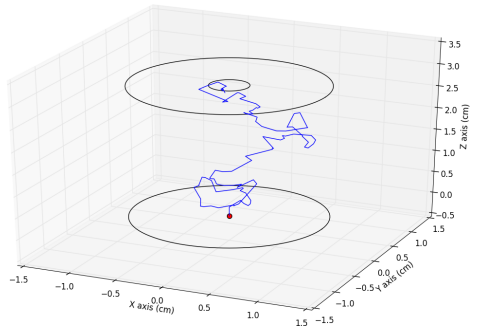

Figure 1: Propagation of an electron in the absence of a magnetic or electric field scattering isotropicallly through a cylinder filled with an attenuated medium of number density 10^{17} and total scattering cross section of 10^{-16}.

2 Beer-Lambert Law

The Beer-Lambert Law quantifies the attenuating intensity of a propagating beam of particles by a scattering and absorbing medium.

2.1 Derivation

The probability of interaction between a propagating particle and an attenuating particle is the ratio of total cross-sectional area of attenuating particles,

to cross-sectional area of the unit volume,

$$p[x, x + dx] = \frac{\sigma n A \, dx}{A} = \sigma n \, dx, \tag{1}$$

where σcm^2 is the total scattering cross section, and ncm^{-1} is the number density of the attenuating medium. Here, we assume that this number density is constant across the length of the medium. Consequently, the change in intensity across dx is proportional to the number density, n.

$$dI = -\sigma n I \, dx. \tag{2}$$

We solve the ordinary differential equation by separation of variables,

$$\int_{I_0}^{I(l)} \frac{dI}{I} = \int_0^l -\sigma n \, dx. \tag{3}$$

The Beer-Lambert Law,

$$I(l) = I_0 \, e^{-\sigma n l}. \tag{4}$$

Generally for N attenuating species with scattering cross-sections and number densities of σ_i and n_i respectively, the Beer-Lambert Law,

$$I(l) = I_0 \, e^{-\sum_{i=1}^{N} \sigma_i n_i l}. \tag{5}$$

3 Simulation of Electron Propagation

We first consider electron propagation within a cylinder of length $3cm$ and radius $1cm$ filled with an attenuating medium with total scattering cross section of $\sigma = 10^{-16} cm^2$ and number density ncm^{-1}. Electrons are initialized from the origin, $\vec{r} = (0, 0, 0)$, and directed along the z-axis, $\vec{\mu} = (0, 0, 1)$, toward the circular aperture across the length of the cylinder. The electron travels the distance of a random step size governed by the Beer-Lambert Law before interacting with an attenuating particle. The electron is randomly scattered, isotropically or anisotropically, before the next step size is randomly sampled. Electrons are terminated after passing through the aperture or colliding with the boundaries of the cylinder. Our model is implemented in Python.

Inverse transform sampling allows for the generation of a random variable, given its cumulative distribution function, in terms of any probability density. We write a desired random variable, such as step size or scattering angle, in terms of uniformly distributed $\xi \in [0, 1]$; Python already provides pseudo-random means for its selection.

3.1 Step Size

We desire method for selecting step size between scattering events. Consider the Beer-Lambert Law as a probability density function of the distance traveled by an unscattered electron before such an event. We normalize the corresponding cumulative distribution function such that $\lim_{s\to\infty} P(x) = 1$ and $0 \leq P(s) = \xi \leq 1$,

$$P(s) = \int_0^s \sigma n e^{-\sigma n x}\, dx. \tag{6}$$

Solving for s, step size, in terms of ξ,

$$s = -\frac{\ln(\xi)}{\sigma n}. \tag{7}$$

3.2 Scattering Direction

Again given the respective cumulative probability density, inverse transform sampling is used to derive means of selection for both isotropic and anisotropic scattering angles. We are interested in the probability of an electron scattering in the direction of a portion of the spherical solid angle. With polar angle $0 \leq \theta \leq \pi$ and azimuthal angle $0 \leq \phi \leq 2\pi$, we consider probability density functions in spherical coordinates,

$$p(\theta, \phi)\, d\theta\, d\phi = \frac{\sin\theta\, d\theta\, d\phi}{4\pi}. \tag{8}$$

As θ and ϕ are independent random variables, we can consider their joint probability density function as a product of their respective probability density functions, $p(\theta, \theta + d\theta)$ and $p(\phi, \phi + d\phi)$; we sample them each separately.

3.2.1 Isotropic Scattering

In the case of isotropic scattering, a particle has an equal probability of scattering in the direction of any portion of the spherical solid angle. We normalize the cumulative distribution function for θ,

$$P(\theta) = \int_0^\pi \frac{\sin\theta}{2}\, d\theta = 1, \tag{9}$$

and for ϕ,

$$P(\phi) = \int_0^{2\pi} \frac{1}{2\pi}\, d\phi = 1. \tag{10}$$

Integrating each and solving for θ and ϕ as done for step size, s, in subsection 3.1, we obtain,

$$\begin{aligned} \theta &= \arccos(1 - 2\xi_1) \\ \phi &= 2\pi\xi_2. \end{aligned} \tag{11}$$

To convert from a spherical to Cartesian coordinate system,

$$\begin{aligned} \mu_x &= \sin\theta\cos\phi \\ \mu_y &= \sin\theta\sin\phi \\ \mu_z &= \cos\theta. \end{aligned} \tag{12}$$

Condensing expressions of θ by writing them in terms of random variable $\mu_z = \cos\theta \in [-1, 1]$, we reach an equivalent isotropic sampling unit vector in Cartesian coordinates,

$$\begin{aligned} \mu_x &= \sqrt{1 - \mu_z^2}\cos 2\pi\xi \\ \mu_y &= \sqrt{1 - \mu_z^2}\sin 2\pi\xi \\ \mu_z &= \mu_z. \end{aligned} \tag{13}$$

3.2.2 Anisotropic Scattering

The assumed anisotropic scattering description is uniform with respect to ϕ. We sample ϕ as before,

$$\phi = 2\pi\xi. \tag{14}$$

We assume the following probability density function with respect to θ,

$$p[\theta, \theta + d\theta] = \frac{d\sigma}{d\Omega}(\theta, \phi) = \frac{1 + \cos\theta}{2}. \tag{15}$$

Again, we normalize the cumulative distribution function and integrate,

$$\begin{aligned} P(\theta) &= \int_0^{\theta} \frac{1 + \cos\theta}{2} \sin\theta\, d\theta \\ &= -\frac{\cos^2\theta}{4} - \frac{\cos\theta}{2} + \frac{3}{4}. \end{aligned} \tag{16}$$

Solving for θ, we reach means for sampling anisotropic scattering angles,

$$\begin{aligned} \theta &= \arccos\left(\frac{1-\sqrt{9+16\,\xi}}{4}\right) \\ \phi &= 2\pi\xi. \end{aligned} \tag{17}$$

It should be realized that these angles describe anisotropic scattering from an incident directional unit vector not necessarily parallel to the z-axis. Consequently, we must derive equations for these new directional unit vectors in the standard Cartesian basis.

3.2.3 Scattering Directional Unit Vectors in the Standard Basis

As noted in 3.2.2, anisotropic scattering occurs relative to the incident directional unit vector,

$$\mu = \big[\mu_x,\, \mu_y,\, \mu_z\big]. \tag{18}$$

Consequently, the scattering directional unit vector at angles θ and ϕ from the incident vector is written by components in a nonstandard basis,

$$\hat{\mu} = (\sin\theta\cos\phi)\,\mu_\perp \times \mu \,+\, (\sin\theta\sin\phi)\,\mu_\perp \,+\, (\cos\theta)\,\mu \tag{19}$$

Where $\mu_\perp$ is some non-unique unit vector perpendicular to μ. For simplicity, we choose $\mu_\perp$ such that it lies in the $x-y$ plane.

$$\mu_\perp = \Big[\frac{-\mu_y}{\sqrt{1-\mu_z}},\, \frac{\mu_x}{\sqrt{1-\mu_z}},\, 0\Big] \tag{20}$$

Thus,

$$\mu_\perp \times \mu = \Big[\frac{\mu_x\mu_z}{\sqrt{1-\mu_z}}, \frac{\mu_y\mu_z}{\sqrt{1-\mu_z}}, \frac{\mu_z^2-1}{\sqrt{1-\mu_z}}\Big] \tag{21}$$

Finally adding components, we reach a desired set of equations for the new scattering directional unit vector.

$$\begin{aligned} \hat{\mu}_x &= \frac{\mu_x\mu_z\sin\theta\cos\phi - \mu_y\sin\theta\sin\phi}{\sqrt{1-\mu_z}} + \mu_x\cos\theta \\ \\ \hat{\mu}_y &= \frac{\mu_y\mu_z\sin\theta\cos\phi + \mu_x\sin\theta\sin\phi}{\sqrt{1-\mu_z}} + \mu_y\cos\theta \\ \\ \hat{\mu}_z &= -\sqrt{1-\mu_z^2}\,\sin\theta\cos\phi + \mu_z\cos\theta. \end{aligned} \tag{22}$$

When $\mu_z \approx 1$, we consider the incident vector as parallel to the z-axis and apply the conversion from spherical to Cartesian coordinates,

$$\begin{aligned} \hat{\mu}_x &= \sin\theta\cos\phi \\ \hat{\mu}_y &= \sin\theta\sin\phi \\ \hat{\mu}_z &= \cos\theta. \end{aligned} \tag{23}$$

When $\mu_z \approx -1$, we again consider the incident vector as parallel to the z-axis and reflect the directional unit vectors in Equation 26.

$$\begin{aligned} \ddot{x} &= \sin\theta\cos\phi \\ \ddot{x} &= -\sin\theta\sin\phi \\ \ddot{x} &= -\cos\theta. \end{aligned} \tag{24}$$

3.3 Magnetic and Electric Fields

For electric field, $\vec{E}$ Vcm^{-1}, and magnetic field, $\vec{B}$ T, we derive a description of the acceleration of an electron,

$$\frac{d\vec{v}}{dt} = \frac{q}{m}\big(\vec{E} + \vec{v} \times \vec{B}\big). \tag{25}$$

Given that both $\vec{E}$ and $\vec{B}$ are parallel to the z-axis implies the differential equations,

$$\begin{aligned} \ddot{x} &= \frac{q|\vec{B}|}{m}\dot{y} \\ \ddot{y} &= -\frac{q|\vec{B}|}{m}\dot{x} \\ \ddot{z} &= \frac{q|\vec{E}|}{m}. \end{aligned} \tag{26}$$

With $\vec{r}(0) = 0$ and $\vec{v}(0) = \vec{v_0}$, we solve the initial value problem,

$$x(t) = \frac{m}{q|\vec{B}|}\Big(-v_{0,y} + v_{0,y}\cos\frac{q|\vec{B}|}{m}t + v_{0,x}\sin\frac{q|\vec{B}|}{m}t\Big) \tag{27}$$

$$y(t) = \frac{m}{q|\vec{B}|}\Big(v_{0,x} - v_{0,x}\cos\frac{q|\vec{B}|}{m}t + v_{0,y}\sin\frac{q|\vec{B}|}{m}t\Big) \tag{28}$$

$$z(t) = \frac{q|\vec{E}|}{2m}t^2 + v_{0,z}t \tag{29}$$

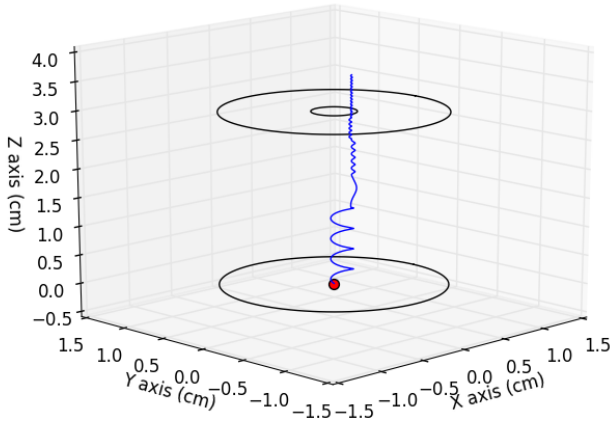

Figure 2: Propagation of an electron in a magnetic field of 0.005 T scattering isotropicallly through a cylinder filled with an attenuated medium of number density 10^{16} and total scattering cross section of 10^{-16}.

4 Simulation of Polarization Experiment

Building on the developed simulation in Section 3, we now consider the attenuating medium as composed of a mixture of Nitrogen molecules and Rubidium atoms. As we derived the step size, s between scattering events before, the Beer-Lambert Law is a probability density function of the distance traveled by an unscattered electron before a scattering event,

$$I(s) = I_0\, e^{-l(\sigma_{Rb} n_{Rb} + \sigma_{N_2} n_{N_2})}, \tag{30}$$

Where σ_{Rb} and σ_{N_2} are the total scattering cross sections of Rubidium and Nitrogen respectively and n_{Rb} and n_{N_2} are the number densities of Rubidium and Nitrogen respectively. In our case, the distance between scattering events is dependent on the energy of the electron. Specifically for our model,

$$\sigma_{N_2} = \begin{cases} 10^{-}15 & \text{if} \quad a < E < b \quad \text{eV} \\ 10^{-}16 & \text{if} \quad E < a,\ b < E \quad \text{eV} \end{cases} \tag{31}$$

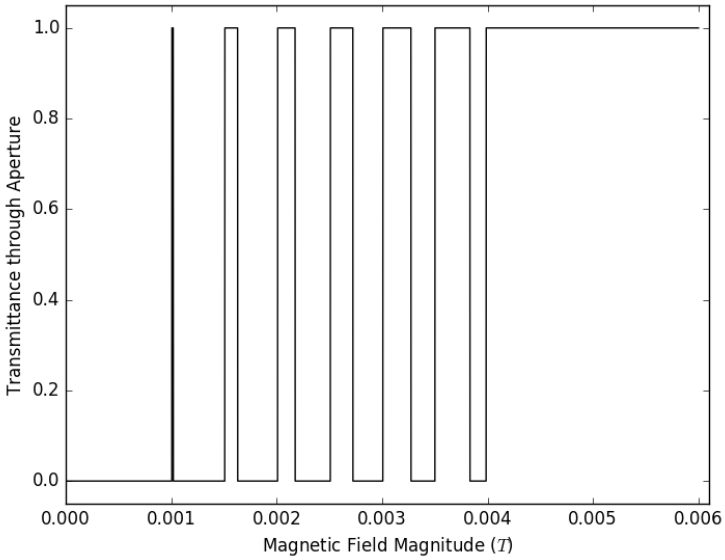

Figure 3: Verifying our derivation, a plot of the magnetic field magnitude vs. transmittance through an aperture of 0.1 cm.

$$\sigma_{Rb} = 10^{-14}\, e^{-v/10^6}. \tag{32}$$

Where E is the energy of the electron in eV and v is the velocity of the electron in m/s.

Given the occurrence of a collision event, the electron has a probability of $(\sigma_{Rb} n_{Rb})/(\sigma_{Rb} n_{Rb} + \sigma_{N_2} n_{N_2})$ having interacted with a Rubidium atom and $(\sigma_{N_2} n_{N_2})/(\sigma_{Rb} n_{Rb} + \sigma_{N_2} n_{N_2})$ with a Nitrogen molecule.

In our model, electrons scatter elastically from a Nitrogen molecule when $a < E < b$ eV and completely inelastically when $E < a$ or $b < E$ eV.

4.1 Velocity of Elastically Scattered Particle

For our model, we assume all Nitrogen gas to be initially motionless. Thus, the Law of Conservation of Momentum dictates that,

$$m_1 v_{1,x} = m_1 v'_{1,x} + m_2 v'_{2,x}, \tag{33}$$

$$m_1 v_{1,y} = m_1 v'_{1,y} + m_2 v'_{2,y}, \tag{34}$$

$$m_1 v_{1,z} = m_1 v'_{1,z} + m_2 v'_{2,z}. \tag{35}$$

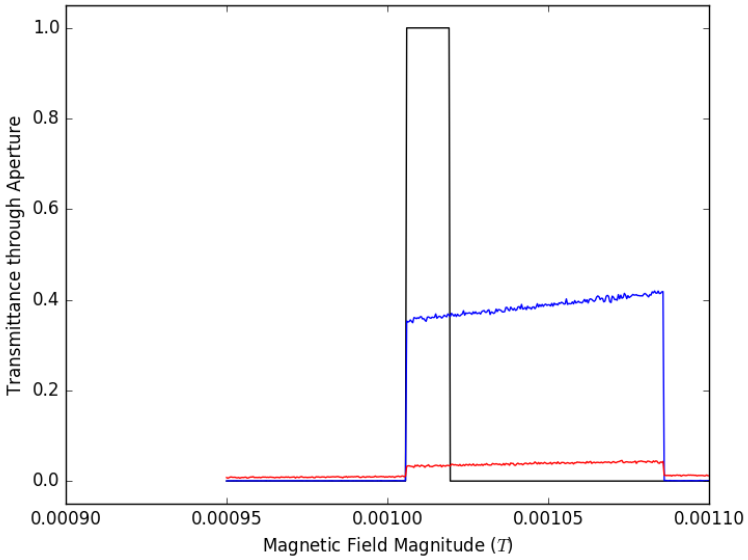

Figure 4: A plot of the magnetic field magnitude vs. transmittance through an aperture of 0.1 cm for number densities of 0 (black), 10^14 (blue), and 10^16.

Where m_1 and m_2 are the masses of the scattering and attenuating particles respectively, v_1 is the incident velocity of the scattering particle, and v_1' and v_2' are the final velocities of the scattering and attenuating particle respectively. Given the scattering angles, θ and ϕ, we rewrite $v_{2,x}'$ and $v_{2,y}'$ in terms of $v_{2,z}'$.

$$m_1 v_{1,x} = m_1 v_{1,x}' + m_2 v_{2,z}' \tan\theta \cos\phi, \tag{36}$$

$$m_1 v_{1,y} = m_1 v_{1,y}' + m_2 v_{2,z}' \tan\theta \sin\phi, \tag{37}$$

$$m_1 v_{1,z} = m_1 v_{1,z}' + m_2 v_{2,z}'. \tag{38}$$

Additionally as the collision is elastic,

$$\frac{m_1 v_1^2}{2} = \frac{m_1 v_1'^2}{2} + \frac{m_2 v_2'^2}{2} \tag{39}$$

Solving for $v_{1,x}'$, $v_{1,x}'$, and $v_{1,x}'$ in (36), (37), and (38) respectively,

$$v_{1,x}' = v_{1,x} - \frac{m_2}{m_1} v_{2,z}' \tan\theta \cos\phi \tag{40}$$

$$v'_{1,y} = v_{1,y} - \frac{m_2}{m_1} v'_{2,z} \tan\theta \sin\phi \tag{41}$$

$$v'_{1,z} = v_{1,z} - \frac{m_2}{m_1} v'_{2,z} \tag{42}$$

substituting into (39), and then solving for $v'_{2,z}$ we reach,

$$v'_{2,z} = \frac{2v_{1,z} + 2\tan\theta(v_{1,x}\cos\phi + v_{1,y}\sin\phi)}{(1+\tan^2\theta)(1+m_2/m_1)} \tag{43}$$

Finally, (43) can be substituted back into (40), (41), and (42), allowing us to compute the final velocity of the scattered particle,

$$v'_1 = v'^2_{1,x} + v'^2_{1,y} + v'^2_{1,z}. \tag{44}$$

5 Results

Applying our Monte Carlo algorithm to our simulation in Section 3, plotting the relationship between number density and aperture transmission verifies, in particular for small aperture radii, our model's approximation to the scattering description of the Beer-Lambert Law. Figure 5, for aperture radii of 0.05 and 0.9, depicts a scatter plot of such a relationship for both linear and logarithmic scales. In order to demonstrate an approximation of the Beer-Lambert Law for small aperture radii, linear least-squares regressions of the logarithmic scaled data points for both aperture sizes are also plotted:

With total scattering cross-section of $\sigma = 10^-16cm^2$ and cylinder length of $l = 3cm$, the regression equation for an aperture of radius 0.05,

$$y = e^{-(2.914\times10^{-16})\,n} \tag{45}$$

The regression equation for an aperture of radius 0.9,

$$y = e^{-(1.678\times10^{-16})\,n} \tag{46}$$

Continuing to compare the Beer-Lambert Law to intensity attenuation in our models across varied apertures, we plot the relationship between aperture radius and the ratio $-\ln(I/I_0)/\sigma nl$. As expected in figure 6, both models of isotropic and anisotropic scattering approach the Beer-Lambert Law for small aperture radii. Corresponding to greater aperture transmittance rates, the value of the ratio, $-\ln(I/I_0)/\sigma nl$, decreases for larger aperture radii for both isotropic (black) and forward-anisotropic (red) scattered electron beams.

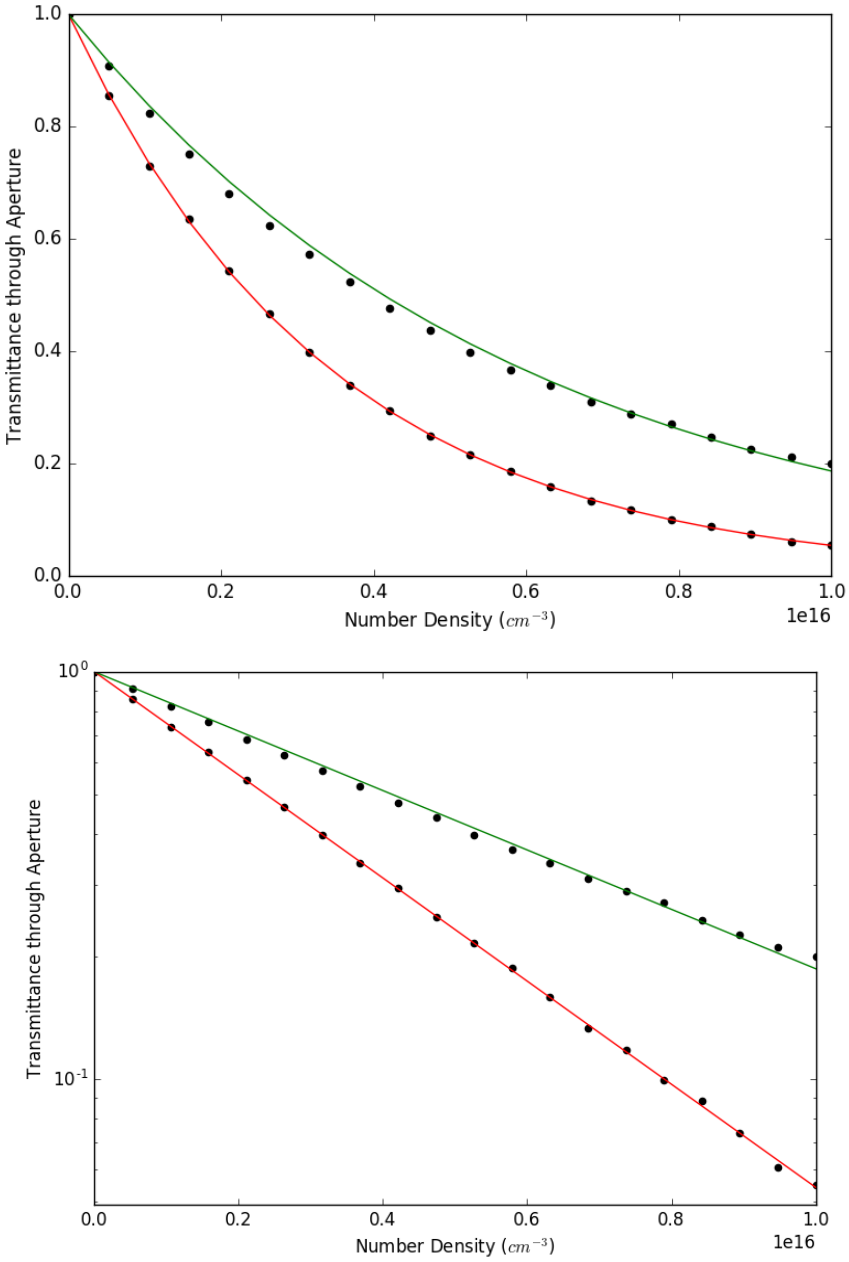

Figure 5: Respectively linear and logarithmic scaled scatter plots of aperture transmittance vs. number density relationships for aperture radii of 0.05 (green) and 0.9 (red). Linear regressions of logarithmic scaled data points are displayed as colored solid lines.

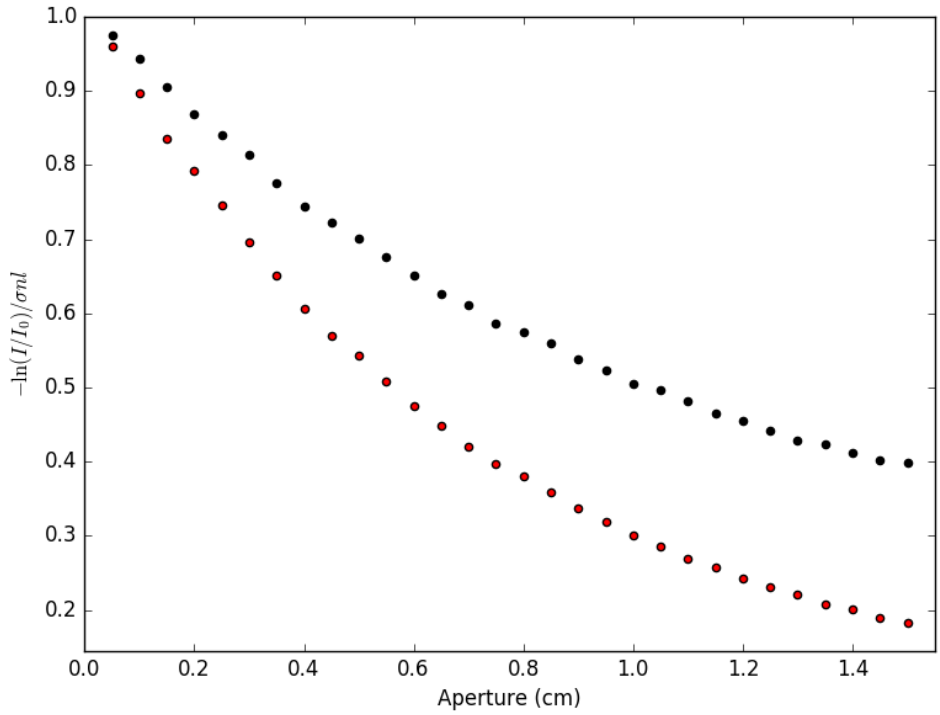

Figure 6: Scatter plot of aperture radius vs. $-\ln(I/I_0)/\sigma nl$ relationship. Data points considering isotropically scattering electrons are black while points considering anisotropic scattering described in subsection 3.2.2 are red.